Chapter

Spacecraft Guidance Sensing at Relativistic Velocities

Emanuele Calabrò

Abstract

In this chapter a solution to the problem of planning an interstellar voyage at relativistic velocities by automatic control was proposed. To this aim, position and velocity of a relativistic interstellar spacecraft can be found by means of automatic measurements onboard of the aberrated angular distances between three quasars, at least. Indeed, this set can represent a reliable inertial reference frame due to the circumstance that quasars can be considered fixed in the space due to their large distances from Earth. To this aim, the so-called apical latitude and longitude of some quasars can be obtained from their right ascension α and declination δ in astronomical catalogues, using some mathematical expressions to provide the aberrated coordinates of a relativistic spacecraft during an interstellar space mission. The algorithm used in this study showed that the accuracy of determining the aberrated apical coordinates of a spacecraft increases significantly using quasars with aberrated apical latitude values lower than 45° in the direction of motion, suggesting that one or more normal-sized telescopes aboard the spacecraft can use quasars within a cone with angular aperture of about 45°, providing aberrated apical latitudes of the spacecraft with errors ranging from 10^{-7} to 10^{-9}.

Keywords: apical aberrated coordinates, quasars, relativistic velocities, interstellar navigation, spherical astronomy, spacecraft automatic control

1. Introduction

The history of human civilization is characterized by a natural tendency of extending the limits of human exploration. This is surely the most important reason of the exploration of interstellar spaces. Furthermore, the exponential increase in energy requirement by mankind may be considered another reason of the exploration of interstellar spaces. Nevertheless, also the research of extraterrestrial life can be considered an input to explore interstellar spaces.

In this regard, several projects to plan an automated spacecraft throwing toward the nearest interstellar systems have been proposed up to now. Project Orion proposed a mission toward the star closest to Earth, Alpha Centauri, using the nuclear pulse propulsion system, a mission which would take about 140 years [1, 2]. Project Daedalus followed the guidelines that the spacecraft could be designed to allow for a variety of target stars, reaching its destination within a human lifetime, using electron-driven D/He_3 fusion reactions, to accelerate the spaceship up to 12% of the velocity of light [3]. Project Icarus has been recently proposed to revise some aspects of the original Project Daedalus, as the choice of fuel to be used as a

propellant [4]. Further possible techniques for propulsion of an interstellar spacecraft have been proposed up to now [5–7]. Nevertheless, an upper limit to the velocity of an interstellar spacecraft exists, because, hypothesizing a velocity comparable to the light velocity, the spaceship will get a weight more than 2000 ton. Hence, a reasonable value of velocity of an interstellar spaceship would not exceed 0.3 c for an interstellar voyage, and it is expected to last about 30 years, at least. Such long time forces us to plan navigation and guidance of the spacecraft by means of automated control on-board the spacecraft. Indeed, sending a signal from a spaceship to Earth at a distance of several light years would ask for an extremely long time, as the signal would travel at the velocity of light, making out of the question any Earth-side control of an interstellar mission.

Otherwise, mankind's exploration of space has been characterized by the extraordinary achievements of both robotic and manned space missions. The success of robotic space missions was due to the development of automated space navigation systems that have enabled the determination of the spacecraft's position and velocity, providing accuracies for traversing interplanetary distances and obtaining precise landings on the surface of the moon and of some planet of the solar system. The required position and velocity of a space mission to support trajectory corrections can be obtained by the current and predicted values of the spacecraft's position and velocity, provided by ground and on-board guidance and control systems.

In contrast, hypothesizing an interstellar voyage, no navigation and guidance control can be carried out by control systems on Earth because of the very long distances between Earth and stars. An interstellar spacecraft should check automatically its trajectory, calculating direction and modulus of its velocity by means of automatic measurements on-board. To this aim, a celestial reference frame is needed so that a fixed coordinate system can provide an instantaneous determination of the spacecraft's position with respect to the celestial reference frame. Hence, the spacecraft's trajectory can be compared with knowledge of the destination stellar object, and maneuver control can be applied, determining velocity changes to rectify the spaceship's trajectory.

Previous studies showed that a celestial reference frame constituted by three quasars, at least, can be successfully used to determine position and velocity of an interstellar spacecraft [8]. Indeed, quasi-stellar objects (quasars) can be considered a reliable inertial reference frame for an interstellar voyage because they are point-like stellar objects and their proper motion can be neglected due to their extremely long distance. Furthermore, the accuracy of determining the aberrated coordinates of an interstellar spacecraft can be improved using a set of quasars whose aberrated apical latitudes are within a cone with an angular aperture of 45° and the axis in the direction of motion of the spacecraft.

2. The celestial reference frame for an interstellar space mission

Previous space missions within the solar systems have been carried out up to now in a space reference frame associated with the planetary ephemeris represented by a solar system barycentric frame aligned with the planetary ephemeris. In previous space missions, space radio tracking has been performed by means of Doppler and range systems and very-long-baseline interferometry (VLBI), so that accurate information regarding corrections to be carried out to the spacecraft's trajectory were obtained [9].

Otherwise, automatic measurements on-board an interstellar spacecraft should be carried out to check the prefixed trajectory, comparing computed values of position and velocity with expected values of position and velocity so that the

spaceship's trajectory can be automatically rectified toward its target. To this aim, the primary step to plan an interstellar space mission is the choice of a reliable inertial reference frame, using computing and motion sensors on-board for tracking spacecraft's position, orientation, and velocity to support trajectory corrections.

The discovery of radio pulsars led to the idea of using pulsar timing observations for interstellar navigation [10]. Indeed, pulsars are rotating neutron stars that emit beams of electromagnetic radiation, and they are bright enough to be used in a space mission. Nevertheless, some limitations reduce their effectiveness in navigation and guidance of interstellar space missions. Indeed, neighboring celestial objects are broadband radio sources that can obscure weak pulsar signals [11]. Furthermore, propagation of radio signals is in phase lags of variable and unpredictable duration so that they set the limitation on accuracy. The most relevant limitation is that at radio frequencies that pulsars emit, radio-based systems on-board would require too large antennas impracticable for a spacecraft. Furthermore, optical observations of pulsars during interstellar navigation would be impractical because of the small number of detectable optical pulsars [10–12].

X-ray pulsars were recently considered to overhead these limitations. Indeed, an X-ray telescope of normal-size dimension can be required to detect X-ray pulsars. The basic concept of interstellar space missions using X-ray pulsars was recently described [12–14]. Nevertheless, other limitations have to be considered. First, long-term observations of X-ray pulsars highlight irregularities in the pulse rate. Second, irregularities in the spacecraft's clock could cause an error in measurement of time of arrivals of pulsars' beam. Third, the pulse shape may differ between the X-ray and the radio wave bands producing an offset between the time of arrivals measured using the different bands. Finally, pulsar timing ephemeris obtained from long-term ground-based radio observations may be not reliable because pulsars' proper motion cannot be negligible and reducing uncertainties that arise from pulsar position errors is critical.

Otherwise, quasars' position can be considered stationary in the sky because of their large distance from the observer, deduced by very high redshift values. Indeed, spectra of the most numerous quasars can be explained only by a cosmological redshift due to the expansion of the universe. The accretion of material on a central, massive black hole can explain the observed high quasar energy fluxes. Hence, quasars can be considered a reliable inertial reference frame because their proper motion can be neglected due to their extreme distance and bright and point-like appearance. As regards this topic, the International Celestial Reference Frame (ICRF) was proposed, and it represents a catalogue of extragalactic radio sources observed with VLBI; the majority of them are quasars and are distributed around the sky [15]. The ICRF was successively developed using an extended list of sources that was adopted by the International Astronomical Union in 2009 for a second realization of a new catalogue named ICRF2, which provides absolute coordinates for 3414 sources with errors within 0.1 mAs (milliarcseconds) and the orientation of the axes that can be considered fixed within 0.01 mAs [16, 17].

Proper motions of sources could be taken into account to improve the reliability of ICRF2. The dominant proper motion of the major parts of sources is related to internal structural changes that can produce apparent motions several 100 μAs/yr (microarcseconds per year), that is, an order of magnitude larger than proper motions due to the secular aberration drift. However, proper motion due to internal structural changes was detected to be relevant only for unstable sources. A selection of stable sources could be made for a realization of a catalogue of quasars to be used for interstellar space missions. Instead, secular aberration drift is an apparent change in the velocity of distant objects caused by the acceleration of the solar system barycenter directed toward the Galactic Center. This effect may cause

apparent proper motion of all quasars by an estimated average value 4–6 μAs/yr and direction toward the points with equatorial coordinates α = 266° and δ = −29° [18]. Also this error may be considered negligible, but it could be taken into account for accurate planning of interstellar space mission.

Hence, quasars can represent a reliable inertial reference frame to be used for interstellar space missions, because their proper motions can be neglected. In the optical domain, the Hipparcos catalog is currently used for optical astrometry, due to the launch in 1989 of the ESA space-astrometry satellite Hipparcos, which was aligned to the ICRF within 0.6 mAs for the orientation at 1991.25. Nevertheless, other ambitious space-astrometry projects will provide astrometry measurements in the optical domain. The ESA Gaia mission, which will survey about 109 stellar objects brighter than 20 magnitude (mag), with expected accuracies in the 7–25 μAs, ranges down to 15 mag and sub-mAs accuracies at the limit 20 mag. The observations of about 500,000 quasars will provide the Gaia extragalactic reference frame (GCRF), a kinematically nonrotating system close to 0.3 μAs/yr and a positional precision reaching 50 μAs. Of these, only the quasars with the most accurate positions with magnitude lesser than 18 will be used to define a new celestial reference frame in the optical domain, the Large Quasar Reference Frame (LQRF) [19]. The final catalogue is expected around 2021, but with intermediate data that are expected to be available by 2015. An accurate alignment between the two celestial reference frames, the LQRF and the ICRF, can be carried out using only 10% of the current ICRF sources for the alignment with the future Gaia frame, but further multistep VLBI observational projects have been planned to observe new VLBI sources suitable for the alignment with the future Gaia frame [19].

Another space-astrometry project is the Space Interferometry Mission PlanetQuest Light (SIM-Lite), which consists of an optical interferometer system with a baseline of 6 m and a 30-cm guide telescope that would search 65 nearby stars for planets of masses down to one Earth mass, achieving 8 μAs accuracy on the nineteenth magnitude objects and 4 μAs for objects up to 14 mag that would constitute a new astrometric grid.

3. The apical coordinate system

The inertial reference frame for interstellar missions can be represented by a spherical coordinate system where the spacecraft is at rest. This system is termed the "apical system" and is represented in **Figure 1**, where the origin of the system represents the position of the spaceship, OV is the direction of the motion, P is the North equatorial pole, and Q is a quasar. The *apical latitude* θ is measured from the direction of the spacecraft's velocity OV to the quasar Q. The *apical longitude* l is measured from the plane that contains the direction of velocity and the direction of the equatorial pole to the plane containing the same vector of velocity and the quasar (see **Figure 1**).

The apical coordinates of a quasar can be related to its astronomical coordinates the *right ascension* α and the *declination* δ (that are known from the ICRF2 catalogue) by means of some equations derived from spherical astronomy [20, 21]:

$$\sin\theta = \sin\delta_v \sin\delta + \cos\delta_v \cos\delta \cos(\alpha_v - \alpha) \tag{1}$$

$$\cos\theta = \frac{\cos\delta \sin(\alpha_v - \alpha)}{\sin l} \tag{2}$$

$$\cos l = \frac{\sin\delta \cos\delta_v - \cos\delta \cos\delta_v \cos(\alpha_v - \alpha)}{\cos\theta} \tag{3}$$

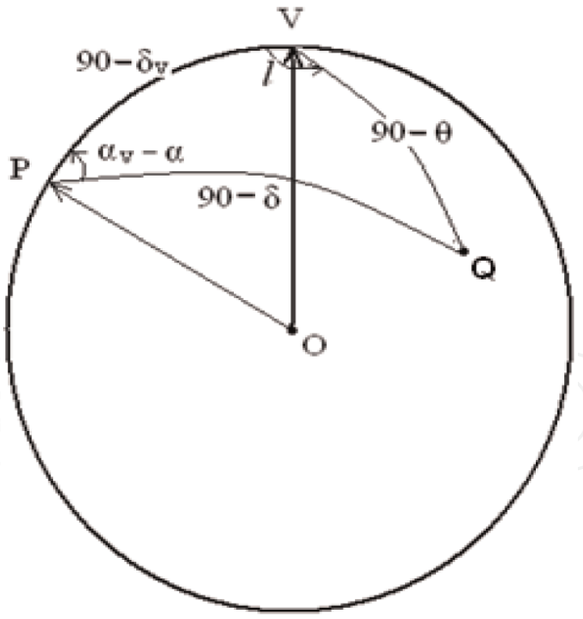

Figure 1.
The apical latitude θ and the apical longitude l of a quasar in the apical system.

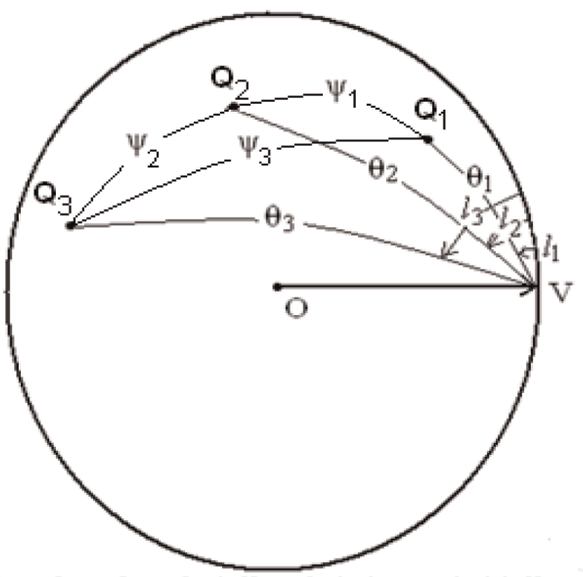

Figure 2.
The apical coordinates θ_i and l_i (i = 1, 2, 3) of three quasars in the apical system (where the spacecraft is at rest).

where α_v and δ_v are the stationary coordinates of the vector velocity of the spacecraft that have to be recomputed during the voyage.

The spaceship should determine its position by means of the apical coordinates of a number of quasars. It was shown that spacecraft's position and velocity can be determined using only three quasars by means of automatic measurements on-board the spacecraft of the angular distances ψ_i between the quasars [8].

Indeed, the angular distances ψ_1, ψ_2, and ψ_3 between three quasars named Q_1, Q_2, and Q_3, pointed out in **Figure 2**, can be related to their apical coordinates applying the II Gauss formula to the spherical triangles represented in **Figure 2**:

$$\cos\psi_1 = \cos\theta_1 \cos\theta_2 + \sin\theta_1 \sin\theta_2 \cos(l_2 - l_1) \tag{4}$$

$$\cos\psi_2 = \cos\theta_3 \cos\theta_2 + \sin\theta_3 \sin\theta_2 \cos(l_3 - l_2) \tag{5}$$

$$\cos\psi_3 = \cos\theta_3 \cos\theta_1 + \sin\theta_3 \sin\theta_1 \cos(l_3 - l_1) \tag{6}$$

Measurements on-board the spaceship of the angular distances ψ_1, ψ_2, and ψ_3 could be used to obtain the apical coordinates, determining the position and velocity of a spacecraft.

4. The aberrated apical coordinates at relativistic velocities

The most relevant effect to be taken into account at relativistic velocities is represented by the change in direction of a stellar object because the point of view of an object from a moving observer depends on its velocity, and this change is not negligible if the velocity is comparable to the velocity of light. Indeed, according to the relativistic aberration, during the motion of an object, its apical coordinates θ_i change into θ_i' as follows [22]:

$$\cos\theta' = \frac{\cos\theta + \beta'}{1 + \beta'\cos\theta} \tag{7}$$

$$\sin\theta' = \frac{\sin\theta}{\gamma\,(1 + \beta'\cos\theta)} \tag{8}$$

where $\beta' = v/c$, $\gamma = 1/\sqrt{1-\beta'^2}$.

(v and c are the velocities of the spacecraft and of light, respectively).

As the velocity of a spacecraft during an interstellar space mission should range from 0.1 to 0.3 c, the apical coordinates θ_i and l_i of the spacecraft (i = 1, 2, 3) and the angular distances ψ_i between the quasars should change in the "aberrated coordinates" θ_i', l_i', and ψ_i', respectively. However, the aberrated coordinates of the spaceship can be related to its apical coordinates applying some relation analogue to Eqs. (4)–(6).

In particular, the spacecraft's velocity value V_{j+1} at the time (j + 1) and the related aberrated coordinates can be obtained from the spacecraft's velocity V_j and the aberrated coordinates at the time (j) by means of measurements of three quasars at least and some expressions derived from spherical astronomy [20, 21]. The apical and aberrated coordinates of the velocities V_1 (j = 1) and V_2 are pointed out in **Figure 3**. The vectors V_1 and V_2 may be represented in the apical system by their apical coordinates $[(\theta_{A,1}, l_{A,1}), (\theta_{B,1}, l_{B,1}), (\theta_{C,1}, l_{C,1})]$ and $[(\theta_{A,2}, l_{A,2}), (\theta_{B,2}, l_{B,2}), (\theta_{C,2}, l_{C,2})]$, respectively.

Nevertheless, only measurements of the aberrated angular distances ψ_i'' (i = 1, 2, 3) between the quasars can be carried out aboard the spacecraft. Applying the II Gauss' formulae to the spherical triangles ABV_2 and $A''B''V_2$, BCV_2 and $B''C''V_2$, and CAV_2 and $C''A''V_2$, the following relations can be obtained:

$$\cos\psi_1'' = \cos\theta_{A_2}'' \cos\theta_{B_2}'' + \sin\theta_{A_2}'' \sin\theta_{B_2}'' \cos E_{2,1}'' \tag{9}$$

$$\cos\psi_2'' = \cos\theta_{B_2}'' \cos\theta_{C_2}'' + \sin\theta_{B_2}'' \sin\theta_{C_2}'' \cos E_{2,2}'' \tag{10}$$

$$\cos\psi_3'' = \cos\theta_{A_2}'' \cos\theta_{C_2}'' + \sin\theta_{A_2}'' \sin\theta_{C_2}'' \cos E_{2,3}'' \tag{11}$$

Assuming that the dihedral angles $E_{i,j}$ (i, j = 1, 2) between two quasars do not change because of their large distances from the observer (i.e., $\cos E_{2,i} = \cos E_{2,i}''$, i = 1, 2, 3), we can relate Eqs. (9)–(11) to analogue expressions where the not-aberrated coordinates appear:

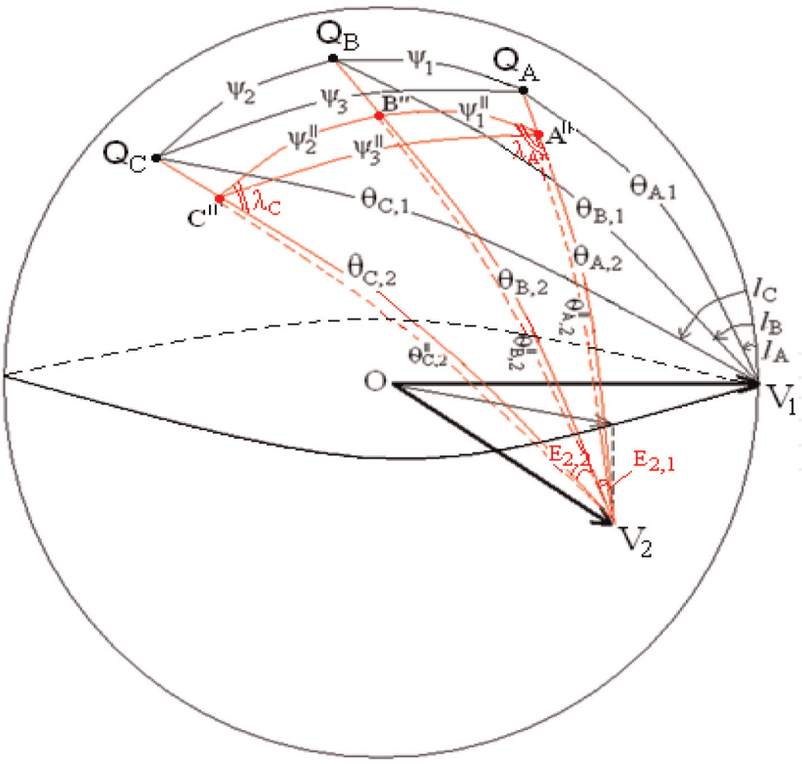

Figure 3.
The apical coordinates of a spacecraft at two velocities V_1 ($\theta_{i,1}$; i = A, B, C) and V_2 ($\theta_{i,2}$; i = A, B, C). The aberrated angular distances ψ_1 , ψ_2 , and ψ_3 between three quasars (Q_A, Q_B, Q_C) and the aberrated coordinates $\theta_{A,2}$, $\theta_{B,2}$, and $\theta_{C,2}$ referred to velocity V_2 are pointed out.

$$\frac{\cos\psi_1'' - \cos\theta_{A_2}'' \cos\theta_{B_2}''}{\sin\theta_{A_2}'' \sin\theta_{B_2}''} = \frac{\cos\psi_1 - \cos\theta_{A_2}\cos\theta_{B_2}}{\sin\theta_{A_2}\sin\theta_{B_2}} \tag{12}$$

$$\frac{\cos\psi_2'' - \cos\theta_{B_2}'' \cos\theta_{C_2}''}{\sin\theta_{B_2}'' \sin\theta_{C_2}''} = \frac{\cos\psi_2 - \cos\theta_{B_2}\cos\theta_{C_2}}{\sin\theta_{B_2}\sin\theta_{C_2}} \tag{13}$$

$$\frac{\cos\psi_3'' - \cos\theta_{A_2}'' \cos\theta_{C_2}''}{\sin\theta_{A_2}'' \sin\theta_{C_2}''} = \frac{\cos\psi_3 - \cos\theta_{C_2}\cos\theta_{A_2}}{\sin\theta_{C_2}\sin\theta_{A_2}} \tag{14}$$

Applying the formulation of the relativistic aberration to the aberrated coordinates θ_{A2}, θ_{B2}'', and θ_{C2}'', the apical coordinates θ_{A2}, θ_{B2}, and θ_{C2} can be obtained, respectively, by means of the following equations, derived from Eqs. (7) and (8):

$$\sin\theta_{A_2}'' = \frac{\sin\theta_{A_2}}{\gamma\left(1+\beta''\cos\theta_{A_2}\right)} \quad \cos\theta_{A_2}'' = \frac{\cos\theta_{A_2}+\beta''}{1+\beta''\cos\theta_{A_2}} \tag{15}$$

$$\sin\theta_{B_2}'' = \frac{\sin\theta_{B_2}}{\gamma\left(1+\beta''\cos\theta_{B_2}\right)} \quad \cos\theta_{B_2}'' = \frac{\cos\theta_{B_2}+\beta''}{1+\beta''\cos\theta_{B_2}} \tag{16}$$

$$\sin\theta_{C_2}'' = \frac{\sin\theta_{C_2}}{\gamma\left(1+\beta''\cos\theta_{C_2}\right)} \quad \cos\theta_{C_2}'' = \frac{\cos\theta_{C_2}+\beta''}{1+\beta''\cos\theta_{C_2}} \tag{17}$$

The set of Eqs. (15)–(17) allows to express the set of Eqs. (12)–(14) as a function of the apical coordinates of the spaceship θ_{A2}, θ_{B2}, and θ_{C2} and of the aberrated modulus of the velocity β″ (in unit of c). Applying again the II Gauss' equation and the sinus theorem to the spherical triangles $B''C''V_2$ and $A''B''V_2$, we obtain

$$\cos\theta''_{B_2} = \cos\psi''_2 \cos\theta''_{C_2} + \sin\psi''_2 \sin\theta''_{C_2} \cos\lambda_C \tag{18}$$

$$\cos\theta''_{B_2} = \cos\psi''_1 \cos\theta''_{A_2} + \sin\psi''_1 \sin\theta''_{A_2} \cos\lambda_A \tag{19}$$

$$\sin\lambda_A = \frac{\sin E_{2,1} \sin\theta''_{B_2}}{\sin\psi''_1} \quad \sin\lambda_C = \frac{\sin E_{2,2} \sin\theta''_{B_2}}{\sin\psi''_2} \tag{20}$$

The set of equations reported above allows to obtain the apical coordinates θ_{A2}, θ_{B2}, and θ_{C2} (at time j = 2) as a function of the apical coordinates θ_{A1}, θ_{B1}, and θ_{C1} (at time j = 1) and of the measured quasars' angular distances ψ_1'', ψ_2'', and ψ_3''. Hence, this algorithm can provide the direction and modulus of velocity that have to be used to rectify the trajectory of the spacecraft toward its target.

5. Applying the algorithm to determine the spacecraft's aberrated apical coordinates

The solution of the set of equations reported above can provide the exact values of the aberrated coordinates of a spaceship that are required for navigation and guidance during an interstellar space mission. Nevertheless, previous results showed that the accuracy of determining the aberrated coordinates depends on the apical coordinates of the quasars that are used. Indeed, it was shown that applying the algorithm to typical apical latitudes around 90° of three quasars, the best accuracy in the determination of apical coordinates can be obtained using quasars with apical longitudinal angular distances around 90° and 180° [8].

In this simulation study, instead of simulating a variation of quasars' apical longitudes, quasars' apical latitudes ranging from 5° to 120° were used, using also the value of the spaceship's aberrated velocity modulus β = 0.1 (in unit of c) and the values $\theta = l$ = 0.5° that represent a typical change in direction of the motion of the spacecraft. The results of this simulation study were reported in **Tables 1–12** (in the Appendix section) where quasars' aberrated angular distances, spacecraft's aberrated apical latitudes, and aberrated velocity modulus values were reported as a function of typical quasars' apical latitudes and longitudes. Looking at the results reported in **Tables 1–12**, it appears that the aberrated velocity modulus values obtained from the input value β'' = 0.1 are all very close to this value, confirming the reliability of the algorithm. In addition, the variations of the aberrated velocity modulus decreased with the decrease of quasars' apical latitude, getting the best accuracy using quasars' aberrated apical latitudes lower than 45°. The average of the values of spacecraft's aberrated velocity modulus obtained at typical apical longitudes was plotted as a function of quasars' aberrated apical latitude, and a sigmoidal fit was used with upper and lower asymptotes equal to 7.08×10^{-7} and 4.88×10^{-8}, respectively (see **Figure 4**). A statistical analysis was carried out applying Student's t-test for comparison between two groups: the group of quasars whose aberrated apical latitude are $\theta \leq 45°$ and the group of quasars with $\theta > 90°$, with $p < 0.05$ considered significant. The t-test provided the result that the group of quasars with $\theta \leq 45°$ is significantly different in comparison to the other group ($p < 0.01$), showing that the accuracy of determining the spacecraft's aberrated velocity β'' increases using quasars' aberrated apical latitude $\theta \leq 45°$. Hence, the result of this simulation study has confirmed that a celestial reference frame consisting of three quasars can be successfully used for interstellar navigation regardless of their apical coordinates, but the best accuracy in the determination of spacecraft's apical coordinates can be obtained using quasars whose aberrated apical latitudes are lower than 45°.

Apical latitudes (deg) $\theta_A = 5; \theta_B = 5; \theta_C = 5$				
Apical longitude values (deg) l_A l_B l_C	**Quasars' aberrated angular distances (rad)** Ψ_1'' Ψ_2'' Ψ_3''	**Aberrated apical latitudes (rad)** θ_{A2}'' θ_{B2}'' θ_{C2}''	**Aberrated velocity** $\beta'' = v''/c$	**Uncertainty of aberrated apical latitudes** $\Delta\theta''$ **(rad)**
0	6.036476×10^{-2}	7.104854×10^{-2}	0.1	1.58638×10^{-9}
45	6.036476×10^{-2}	7.352113×10^{-2}		
90	0.1115786	7.104854×10^{-2}		
0	0.1366982	7.104854×10^{-2}	0.1	9.794508×10^{-9}
120	0.1366982	8.311642×10^{-2}		
240	0.1366908	7.104854×10^{-2}		
0	0.1572874	7.104854×10^{-2}	0.1	7.521397×10^{-8}
170	0.1400199	8.672082×10^{-2}		
45	6.036476×10^{-2}	7.351951×10^{-2}		
45	0.157287	7.352113×10^{-2}	0.1	5.19094×10^{-7}
215	0.1400161	8.377577×10^{-2}		
90	6.036476×10^{-2}	7.104854×10^{-2}		
90	6.03667×10^{-2}	7.926836×10^{-2}	0.1	1.489584×10^{-9}
45	0.1115813	7.352033×10^{-2}		
135	6.03667×10^{-2}	7.362574×10^{-2}		
135	0.1115866	8.466642×10^{-2}	0.1	4.037413×10^{-9}
45	0.1458454	7.352113×10^{-2}		
180	0.0603697	7.940599×10^{-2}		
225	0.1458474	8.475729×10^{-2}	0.1	1.405048×10^{-8}
90	0.1115829	7.104854×10^{-2}		
0	0.1458528	7.927288×10^{-2}		
180	0.1458503	8.684048×10^{-2}	0.1	1.168942×10^{-8}
45	6.036476×10^{-2}	7.352113×10^{-2}		
90	0.1115866	7.104854×10^{-2}		

Table 1.
Quasars' aberrated angular distances, spacecraft's aberrated apical latitudes, uncertainties, and aberrated velocity as a function of quasars' apical latitudes $\theta_A = \theta_B = \theta_C = 5°$.

Apical latitudes (deg) $\theta_A = 10; \theta_B = 10; \theta_C = 10$				
Apical longitude values (deg) l_A l_B l_C	**Quasars' aberrated angular distances (rad)** Ψ_1'' Ψ_2'' Ψ_3''	**Aberrated apical latitudes (rad)** θ_{A2}'' θ_{B2}'' θ_{C2}''	**Aberrated velocity** $\beta'' = v''/c$	**Uncertainty of aberrated apical latitudes** $\Delta\theta''$ **(rad)**
0	0.1204418	0.1500399	0.1	3.873324×10^{-9}
45	0.1204418	0.1524055		
90	0.2228695	0.1500403		
0	0.2732715	0.1500399	0.1	1.859782×10^{-8}
120	0.2732715	0.1619809		
240	0.2732428	0.1500399		
0	0.3146759	0.1500399	0.1	1.405435×10^{-7}
170	0.2799516	0.1657227		
45	0.1204418	0.1524067		

Apical latitudes (deg) $\theta_A = 10; \theta_B = 10; \theta_C = 10$				
Apical longitude values (deg) l_A l_B l_C	**Quasars' aberrated angular distances (rad)** Ψ_1'' Ψ_2'' Ψ_3''	**Aberrated apical latitudes (rad)** θ_{A2}'' θ_{B2}'' θ_{C2}''	**Aberrated velocity** $\beta'' = v''/c$	**Uncertainty of aberrated apical latitudes** $\Delta\theta''$ **(rad)**
45	0.3146734	0.1524059	0.1	2.326587×10^{-7}
215	0.279938	0.1626599		
90	0.1204418	0.1500399		
90	0.1204502	0.1580701	0.1000007	3.756036×10^{-9}
45	0.2228789	0.1524059		
135	0.1204502	0.1525068		
135	0.2229005	0.1635804	0.1	7.86745×10^{-9}
45	0.2916495	0.1524059		
180	0.1204621	0.1582079		
225	0.2916580	0.1636748	0.1	2.711515×10^{-8}
90	0.2228851	0.1500399		
0	0.2916783	0.1580879		
180	0.2916696	0.1658484	0.1	2.471196×10^{-8}
45	0.1204418	0.1524059		
90	0.2229005	0.1500399		

Table 2.
Quasars' aberrated angular distances, spacecraft's aberrated apical latitudes, uncertainties, and aberrated velocity as a function of quasars' apical latitudes $\theta_A = \theta_B = \theta_C = 10°$.

Apical latitudes (deg) $\theta_A = 20; \theta_B = 20; \theta_C = 20$				
Apical longitude values (deg) l_A l_B l_C	**Quasars' aberrated angular distances (rad)** Ψ_1'' Ψ_2'' Ψ_3''	**Aberrated apical latitudes (rad)** θ_{A2}'' θ_{B2}'' θ_{C2}''	**Aberrated velocity** $\beta'' = v''/c$	**Uncertainty of aberrated apical latitudes** $\Delta\theta''$ **(rad)**
0	0.2385968	0.3083875	0.1	8.906437×10^{-9}
45	0.2385968	0.3107102		
90	0.4434312	0.3083873		
0	0.5454995	0.3083875	0.1	3.621693×10^{-8}
120	0.5454995	0.3203031		
240	0.5453854	0.3083873		
0	0.6301567	0.3083875	0.1	2.721964×10^{-7}
170	0.5591298	0.3241316		
45	0.2385968	0.3107106		
45	0.6301463	0.3107102	0.1	3.33884×10^{-7}
215	0.5590756	0.3209947		
90	0.2385968	0.3083875		
90	0.2386291	0.3163490	0.1000001	8.764387×10^{-9}
45	0.4434671	0.3107102		
135	0.2386296	0.3108094		
135	0.4435533	0.3219346	0.1	1.532988×10^{-8}
45	0.5829566	0.3107102		
180	0.2386760	0.3164873		

Apical latitudes (deg) $\theta_A = 20; \theta_B = 20; \theta_C = 20$				
Apical longitude values (deg) l_A l_B l_C	**Quasars' aberrated angular distances (rad)** Ψ_1'' Ψ_2'' Ψ_3''	**Aberrated apical latitudes (rad)** θ_{A2}'' θ_{B2}'' θ_{C2}''	**Aberrated velocity** $\beta'' = v''/c$	**Uncertainty of aberrated apical latitudes** $\Delta\theta''$ **(rad)**
225	0.5829908	0.3220308	0.1	5.315188×10^{-8}
90	0.4434926	0.3083875		
0	0.5830727	0.3164183		
180	0.5830376	0.3242611	0.1000005	5.07998×10^{-8}
45	0.2385965	0.3107100		
90	0.4435540	0.3083875		

Table 3.
Quasars' aberrated angular distances, spacecraft's aberrated apical latitudes, uncertainties, and aberrated velocity as a function of quasars' apical latitudes $\theta_A = \theta_B = \theta_C = 20°$.

Apical latitudes (deg) $\theta_A = 30; \theta_B = 30; \theta_C = 30$				
Apical longitude values (deg) l_A l_B l_C	**Quasars' aberrated angular distances (rad)** Ψ_1'' Ψ_2'' Ψ_3''	**Aberrated apical latitudes (rad)** θ_{A2}'' θ_{B2}'' θ_{C2}''	**Aberrated velocity** $\beta'' = v''/c$	**Uncertainty of aberrated apical latitudes** $\Delta\theta''$ **(rad)**
0	0.3521147	0.4675786	0.1000003	1.502422×10^{-8}
45	0.3521147	0.4698990		
90	0.6590953	0.4675784		
0	0.8153257	0.4675787	0.1	5.38223×10^{-8}
120	0.8153257	0.4795486		
240	0.8150669	0.4675787		
0	0.9472179	0.4675787	0.1	4.057065×10^{-7}
170	0.8364417	0.4834285		
45	0.3521149	0.4699020		
45	0.9471941	0.4698993	0.1	4.579924×10^{-7}
215	0.8363186	0.4802482		
90	0.3521149	0.4675791		
90	0.3521857	0.4755584	0.1	1.484936×10^{-8}
45	0.6591761	0.4698993		
135	0.3521866	0.4699984		
135	0.6593686	0.4811999	0.1	2.243538×10^{-8}
45	0.8733605	0.4698993		
180	0.3522882	0.4756976		
225	0.8734387	0.4812975	0.1	7.921381×10^{-8}
90	0.6592328	0.4675787		
0	0.8736262	0.4756282		
180	0.8735464	0.4835601	0.1	7.698898×10^{-8}
45	0.3521149	0.4698993		
90	0.6593703	0.4675786		

Table 4.
Quasars' aberrated angular distances, spacecraft's aberrated apical latitudes, uncertainties, and aberrated velocity as a function of quasars' apical latitudes $\theta_A = \theta_B = \theta_C = 30°$.

Apical latitudes (deg) $\theta_A = 40; \theta_B = 40; \theta_C = 40$				
Apical longitude values (deg) l_A l_B l_C	**Quasars' aberrated angular distances (rad)** Ψ_1'' Ψ_2'' Ψ_3''	**Aberrated apical latitudes (rad)** θ_{A2}'' θ_{B2}'' θ_{C2}''	**Aberrated velocity** $\beta'' = v''/c$	**Uncertainty of aberrated apical latitudes** $\Delta\theta''$ **(rad)**
0	0.4584757	0.6280316	0.1000001	2.306603×10^{-8}
45	0.4584757	0.6303636		
90	0.8665489	0.6280315		
0	1.080622	0.6280316	0.1000001	7.157303×10^{-8}
120	1.080622	0.6400977		
240	1.080156	0.6280323		
0	1.266572	0.6280316	0.1	5.437029×10^{-7}
170	1.110074	0.6440277		
45	0.4584759	0.6303676		
45	1.266527	0.6303637	0.1	5.889684×10^{-7}
215	1.109851	0.640806		
90	0.4584759	0.6280328		
90	0.4585961	0.6360657	0.1000002	2.284043×10^{-8}
45	0.8666899	0.6303634		
135	0.4585977	0.6304636		
135	0.867028	0.6417693	0.1	2.902025×10^{-8}
45	1.161710	0.6303636		
180	0.4587704	0.6362065		
225	1.161853	0.6418682	0.1	1.05652×10^{-7}
90	0.8667899	0.6280316		
0	1.162195	0.6361363		
180	1.162049	0.6441610	0.1000003	1.036194×10^{-7}
45	0.4584756	0.6303634		
90	0.8670309	0.6280313		

Table 5.
Quasars' aberrated angular distances, spacecraft's aberrated apical latitudes, uncertainties, and aberrated velocity as a function of quasars' apical latitudes $\theta_A = \theta_B = \theta_C = 40°$.

Apical latitudes (deg) $\theta_A = 45; \theta_B = 45; \theta_C = 45$				
Apical longitude values (deg) l_A l_B l_C	**Quasars' aberrated angular distances (rad)** Ψ_1'' Ψ_2'' Ψ_3''	**Aberrated apical latitudes (rad)** θ_{A2}'' θ_{B2}'' θ_{C2}''	**Aberrated velocity** $\beta'' = v''/c$	**Uncertainty of aberrated apical latitudes** $\Delta\theta''$ **(rad)**
0	0.5081233	0.7088562	0.1000001	2.821275×10^{-8}
45	0.5081233	0.7111977		
90	0.9658515	0.7088549		
0	1.210536	0.7088562	0.1	8.064029×10^{-8}
120	1.210536	0.7209837		
240	1.209941	0.7088549		
0	1.427298	0.7088562	0.1000001	6.160802×10^{-7}
170	1.244587	0.7249402		
45	0.5081232	0.7111935		

Apical latitudes (deg) $\theta_A = 45; \theta_B = 45; \theta_C = 45$				
Apical longitude values (deg) l_A l_B l_C	**Quasars' aberrated angular distances (rad)** Ψ_1'' Ψ_2'' Ψ_3''	**Aberrated apical latitudes (rad)** θ_{A2}'' θ_{B2}'' θ_{C2}''	**Aberrated velocity** $\beta'' = v''/c$	**Uncertainty of aberrated apical latitudes** $\Delta\theta''$ **(rad)**
45	1.427240	0.7111977	0.1	6.578899×10^{-7}
215	1.244302	0.7216963		
90	0.5081233	0.7088572		
90	0.5082715	0.7169275	0.1000002	2.795166×10^{-8}
45	0.9660284	0.7111976		
135	0.5082732	0.7112963		
135	0.9664523	0.7226662	0.1	3.206421×10^{-8}
45	1.304455	0.7111977		
180	0.5084859	0.7170680		
225	1.304639	0.7227656	0.1	1.192555×10^{-7}
90	0.9661539	0.7088564		
0	1.305079	0.7169986		
180	1.304891	0.7250745	0.1000001	1.173458×10^{-7}
45	0.5081232	0.7111977		
90	0.9664560	0.7088549		

Table 6.
Quasars' aberrated angular distances, spacecraft's aberrated apical latitudes, uncertainties, and aberrated velocity as a function of quasars' apical latitudes $\theta_A = \theta_B = \theta_C = 45°$.

Apical latitudes (deg) $\theta_A = 55; \theta_B = 55; \theta_C = 55$				
Apical longitude values (deg) l_A l_B l_C	**Quasars' aberrated angular distances (rad)** Ψ_1'' Ψ_2'' Ψ_3''	**Aberrated apical latitudes (rad)** θ_{A2}'' θ_{B2}'' θ_{C2}''	**Aberrated velocity** $\beta'' = v''/c$	**Uncertainty of aberrated apical latitudes** $\Delta\theta''$ **(rad)**
0	0.5985235	0.8719386	0.1	4.217321×10^{-8}
45	0.5985235	0.8743041		
90	1.152048	0.8719379		
0	1.461552	0.8719386	0.1000001	9.980699×10^{-8}
120	1.461552	0.8842108		
240	1.460648	0.871938		
0	1.751104	0.8719386	0.1	7.747448×10^{-7}
170	1.505919	0.8882255		
45	0.5985236	0.8743089		
45	1.751009	0.8743038	0.1000006	8.090532×10^{-7}
215	1.505481	0.8849332		
90	0.5985233	0.8719363		
90	0.5987303	0.8801010	0.1	4.180844×10^{-8}
45	1.152306	0.8743043		
135	0.5987327	0.8744049		
135	1.152921	0.8859171	0.1000003	3.75483×10^{-8}
45	1.584652	0.8743041		
180	0.5990289	0.8802433		

Apical latitudes (deg) $\theta_A = 55; \theta_B = 55; \theta_C = 55$				
Apical longitude values (deg) l_A l_B l_C	**Quasars' aberrated angular distances (rad)** Ψ_1'' Ψ_2'' Ψ_3''	**Aberrated apical latitudes (rad)** θ_{A2}'' θ_{B2}'' θ_{C2}''	**Aberrated velocity** $\beta'' = v''/c$	**Uncertainty of aberrated apical latitudes** $\Delta\theta''$ **(rad)**
225	1.584939	0.8860181	0.1000002	1.483053×10^{-7}
90	1.152488	0.8719386		
0	1.585625	0.8801725		
180	1.585333	0.8883619	0.1	1.467092×10^{-7}
45	0.5985235	0.8743042		
90	1.152927	0.871938		

Table 7.
Quasars' aberrated angular distances, spacecraft's aberrated apical latitudes, uncertainties, and aberrated velocity as a function of quasars' apical latitudes $\theta_A = \theta_B = \theta_C = 55°$.

Apical latitudes (deg) $\theta_A = 65; \theta_B = 65; \theta_C = 65$				
Apical longitude values (deg) l_A l_B l_C	**Quasars' aberrated mangular distances (rad)** Ψ_1'' Ψ_2'' Ψ_3''	**Aberrated apical latitudes (rad)** θ_{A2}'' θ_{B2}'' θ_{C2}''	**Aberrated velocity** $\beta'' = v''/c$	**Uncertainty of aberrated apical latitudes** $\Delta\theta''$ **(rad)**
0	0.6744785	1.037221	0.1000003	6.49072×10^{-8}
45	0.6744785	1.039617		
90	1.31547	1.037223		
0	1.693532	1.037222	0.1	1.224615×10^{-7}
120	1.693532	1.049665		
240	1.692253	1.037221		
0	2.078023	1.037221	0.1000006	9.741514×10^{-7}
170	1.74993	1.053743		
45	0.674478	1.039607		
45	2.077874	1.039617	0.1000002	9.992526×10^{-7}
215	1.749306	1.050399		
90	0.6744784	1.037222		
90	0.6747422	1.045493	0.1000002	6.436005×10^{-8}
45	1.315813	1.039617		
135	0.6747456	1.039722		
135	1.316635	1.051398	0.1000002	4.208667×10^{-8}
45	1.851687	1.039617		
180	0.6751235	1.045640		
225	1.852109	1.051501	0.1000004	1.831758×10^{-7}
90	1.316056	1.037221		
0	1.853118	1.045566		
180	1.852688	1.053883	0.1000002	1.820385×10^{-7}
45	0.6744785	1.039617		
90	1.316643	1.037223		

Table 8.
Quasars' aberrated angular distances, spacecraft's aberrated apical latitudes, uncertainties, and aberrated velocity as a function of quasars' apical latitudes $\theta_A = \theta_B = \theta_C = 65°$.

Apical latitudes (deg) $\theta_A = 75; \theta_B = 75; \theta_C = 75$				
Apical longitude values (deg) l_A l_B l_C	**Quasars' aberrated angular distances (rad)** Ψ_1'' Ψ_2'' Ψ_3''	**Aberrated apical latitudes (rad)** θ_{A2}'' θ_{B2}'' θ_{C2}''	**Aberrated velocity** $\beta'' = v''/c$	**Uncertainty of aberrated apical latitudes** $\Delta\theta''$ **(rad)**
0	0.7328074	1.205014	0.1	1.086075×10^{-7}
45	0.7328074	1.207440		
90	1.446703	1.205018		
0	1.892254	1.205014	0.1	1.559243×10^{-7}
120	1.892254	1.217651		
240	1.890555	1.205017		
0	2.406806	1.205014	0.1000002	1.289855×10^{-6}
170	1.962084	1.221801		
45	0.7328069	1.207434		
45	2.406558	1.207444	0.1000001	1.301131×10^{-6}
215	1.961239	1.218397		
90	0.7328073	1.205012		
90	0.7331199	1.213411	0.1000007	1.076865×10^{-7}
45	1.447127	1.207444		
135	0.7331235	1.207545		
135	1.448146	1.219414	0.1000007	4.551616×10^{-8}
45	2.091397	1.207444		
180	0.7335716	1.213555		
225	2.091990	1.219517	0.1000006	2.351534×10^{-7}
90	1.447428	1.205014		
0	2.093409	1.213484		
180	2.092804	1.221941	0.1000006	2.348527×10^{-7}
45	0.7328073	1.207444		
90	1.448155	1.205017		

Table 9.
Quasars' aberrated angular distances, spacecraft's aberrated apical latitudes, uncertainties, and aberrated velocity as a function of quasars' apical latitudes $\theta_A = \theta_B = \theta_C = 75°$.

Apical latitudes (deg) $\theta_A = 90; \theta_B = 90; \theta_C = 90$				
Apical longitude values (deg) l_A l_B l_C	**Quasars' aberrated angular distances (rad)** Ψ_1'' Ψ_2'' Ψ_3''	**Aberrated apical latitudes (rad)** θ_{A2}'' θ_{B2}'' θ_{C2}''	**Aberrated velocity** $\beta'' = v''/c$	**Uncertainty of aberrated apical latitudes** $\Delta\theta''$ **(rad)**
0	0.7806323	1.46195	0.1000006	4.35259×10^{-7}
45	0.7806323	1.464438		
90	1.559071	1.461949		
0	2.076409	1.461950	0.1000007	3.782526×10^{-7}
120	2.076409	1.474906		
240	2.074203	1.461950		
0	2.875982	1.461950	0.1000005	3.594844×10^{-6}
170	2.163023	1.479170		
45	0.7806325	1.464444		

Apical latitudes (deg) $\theta_A = 90; \theta_B = 90; \theta_C = 90$				
Apical longitude values (deg) l_A l_B l_C	**Quasars' aberrated angular distances (rad)** Ψ_1'' Ψ_2'' Ψ_3''	**Aberrated apical latitudes (rad)** θ_{A2}'' θ_{B2}'' θ_{C2}''	**Aberrated velocity** $\beta'' = v''/c$	**Uncertainty of aberrated apical latitudes** $\Delta\theta''$ **(rad)**
45	2.875224	1.464438	0.1000002	3.465266×10^{-6}
215	2.161893	1.475672		
90	0.7806324	1.461953		
90	0.7809882	1.470553	0.1000007	4.313473×10^{-7}
45	1.559575	1.464438		
135	0.7809924	1.464544		
135	1.560786	1.476717	0.1000008	4.824766×10^{-8}
45	2.330901	1.464438		
180	0.7815026	1.470704		
225	2.331752	1.476824	0.1000007	5.535144×10^{-7}
90	1.559933	1.461950		
0	2.333790	1.470629		
180	2.332921	1.479315	0.1000007	5.63842×10^{-7}
45	0.78063222	1.464438		
90	1.560797	1.461949		

Table 10.
Quasars' aberrated angular distances, spacecraft's aberrated apical latitudes, uncertainties, and aberrated velocity as a function of quasars' apical latitudes $\theta_A = \theta_B = \theta_C = 90°$.

Apical latitudes (deg) $\theta_A = 105; \theta_B = 105; \theta_C = 105$				
Apical longitude values (deg) l_A l_B l_C	**Quasars' aberrated angular distances (rad)** Ψ_1'' Ψ_2'' Ψ_3''	**Aberrated apical latitudes (rad)** θ_{A2}'' θ_{B2}'' θ_{C2}''	**Aberrated velocity** $\beta'' = v''/c$	**Uncertainty of aberrated apical latitudes** $\Delta\theta''$ **(rad)**
0	0.7737214	−1.415936	0.1000007	3.270342×10^{-7}
45	0.7737214	−1.413387		
90	1.542527	−1.415934		
0	2.048211	−1.415936	0.1000008	8.354338×10^{-8}
120	2.048211	−1.402644		
240	2.046092	−1.415936		
0	2.770738	−1.415936	0.1000007	1.055704×10^{-6}
170	2.131879	−1.398259		
45	0.7737212	−1.413391		
45	2.770202	−1.413387	0.1000008	1.061392×10^{-6}
215	2.130802	−1.401856		
90	0.7737214	−1.415935		
90	0.7740707	−1.407115	0.1000007	3.237373×10^{-7}
45	1.543019	−1.413387		
135	0.7740752	−1.413275		
135	1.544199	−1.400782	0.1000006	4.780046×10^{-8}
45	2.292566	−1.413387		
180	0.7745759	−1.406957		

Apical latitudes (deg) $\theta_A = 105; \theta_B = 105; \theta_C = 105$				
Apical longitude values (deg) l_A l_B l_C	**Quasars' aberrated angular distances (rad)** Ψ_1'' Ψ_2'' Ψ_3''	**Aberrated apical latitudes (rad)** θ_{A2}'' θ_{B2}'' θ_{C2}''	**Aberrated velocity** $\beta'' = v''/c$	**Uncertainty of aberrated apical latitudes** $\Delta\theta''$ **(rad)**
225	2.293366	−1.400672	0.1000007	1.896711×10^{-7}
90	1.543368	−1.415936		
0	2.295284	−1.407037		
180	2.294466	−1.398109	0.1000007	1.861201×10^{-7}
45	0.7737215	−1.413387		
90	1.544210	−1.415934		

Table 11.
Quasars' aberrated angular distances, spacecraft's aberrated apical latitudes, uncertainties, and aberrated velocity as a function of quasars' apical latitudes $\theta_A = \theta_B = \theta_C = 105°$.

Apical latitudes (deg) $\theta_A = 120; \theta_B = 120; \theta_C = 120$				
Apical longitude values (deg) l_A l_B l_C	**Quasars' aberrated angular distances (rad)** Ψ_1'' Ψ_2'' Ψ_3''	**Aberrated apical latitudes (rad)** θ_{A2}'' θ_{B2}'' θ_{C2}''	**Aberrated velocity** $\beta'' = v''/c$	**Uncertainty of aberrated apical latitudes** $\Delta\theta''$ **(rad)**
0	0.7084652	−1.145326	0.1000007	1.25511×10^{-7}
45	0.7084652	−1.142719		
90	1.391237	−1.145329		
0	1.806544	−1.145326	0.1000007	1.622084×10^{-8}
120	1.806544	−1.131707		
240	1.805039	−1.145324		
0	2.256094	−1.145326	0.1000007	8.497113×10^{-8}
170	1.870123	−1.127201		
45	0.7084649	−1.142729		
45	2.255899	−1.142719	0.1000008	8.359305×10^{-8}
215	1.869381	−1.130897		
90	0.7084652	−1.145327		
90	0.7087568	−1.136293	0.1000006	1.239996×10^{-7}
45	1.391625	−1.142719		
135	0.7087601	−1.142611		
135	1.392558	−1.129794	0.1000007	4.385023×10^{-8}
45	1.986321	−1.142719		
180	0.7091784	−1.136131		
225	1.986831	−1.129681	0.1000007	9.03231×10^{-10}
90	1.391901	−1.145327		
0	1.988053	−1.136214		
180	1.987532	−1.127048	0.1000007	1.083175×10^{-9}
45	0.7084652	−1.142719		
90	1.392566	−1.145324		

Table 12.
Quasars' aberrated angular distances, spacecraft's aberrated apical latitudes, uncertainties, and aberrated velocity as a function of quasars' apical latitudes $\theta_A = \theta_B = \theta_C = 120°$.

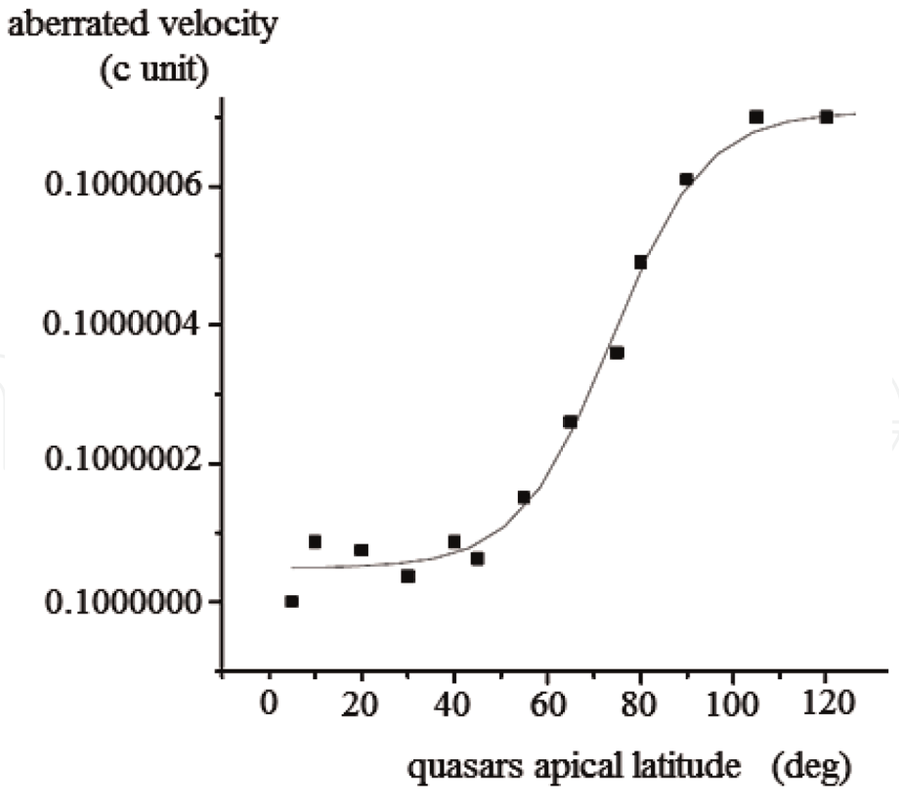

Figure 4.
The averaged aberrated velocity β (in c unit) of a relativistic interstellar spacecraft (with β = 0.1) as a function of quasars' aberrated apical latitude.

Furthermore, as the aberrated coordinates of an interstellar spaceship are related to its aberrated velocity by means of Eqs. (15)–(17) the minimization of the uncertainty in the determination of the spacecraft's aberrated velocity provides an increase in accuracy of determining the aberrated apical coordinates using quasars in that range of aberrated apical latitudes.

This result suggests that one or more normal-sized telescopes aboard the spacecraft can carry out feasible maneuvers along the direction of motion of the spaceship for the automatic measurements of quasars' angular distances because quasars to be used are within a cone with the axis in the direction of motion of the spaceship and an angular aperture of 45° (see **Figure 5**). The large number of quasars whose coordinates have been measured in radio and optical domains and quasars' uniform distribution over the sky [17, 19] can ensure the feasibility of this design.

Furthermore, the limit of accuracy of determining the aberrated coordinates and velocity of an interstellar spacecraft depends on the technique which can be used aboard the spaceship for measuring angular distances between quasars. As described in the previous sections, a positional precision close to 50 μAs for quasars with magnitude lesser than 18 should be reached by means of Gaia space mission which will define a new celestial reference frame in the optical domain, the LQRF. We have performed a simulation study assuming that angular measurements between quasars can be carried out on-board the spaceship with errors within 1 mAs. It may be considered a reasonable estimate of accuracy of automatic angular measurements aboard an interstellar spacecraft, because it represents a value conservatively much smaller than that will be reached in the future astrometry space missions mentioned above. In addition, coordinates' evolution of "stable" quasars is assumed to be around 0.2 mAs [19], so that this uncertainty cannot influence measurements of quasars' angular distance aboard the spacecraft within the assumed accuracy of 1 mAs.

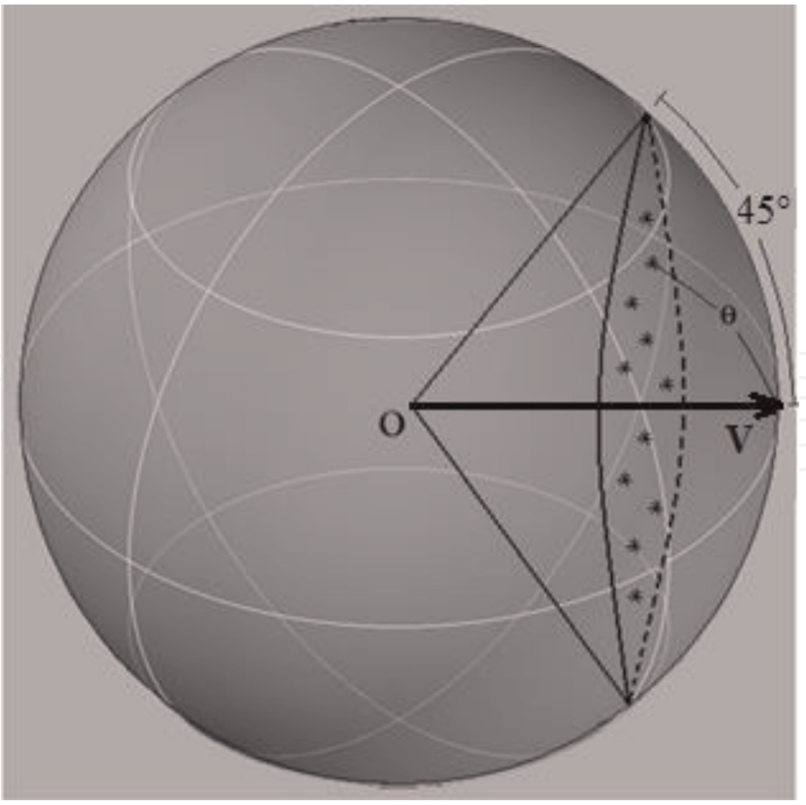

Figure 5.
The accuracy of determining the spacecraft's aberrated velocity and apical coordinates increases using quasars' aberrated apical latitude within a cone with the axis in the direction of motion of the spaceship and an angular aperture of 45°.

Hence, the uncertainty of spacecraft's aberrated apical latitude can be related to the errors of angular measurements carried out on-board the spaceship by means of the following equation derived from Eqs. (18)–(20):

$$\Delta\theta'' = \frac{(\cos\lambda \sin\psi\, \Delta\lambda + \sin\lambda \cos\psi\, \Delta\psi) \sin E - \cos E \sin\lambda \sin\psi\, \Delta E}{\cos\theta'' \sin E^2} \tag{21}$$

The uncertainty values $\Delta\theta''$ of the aberrated apical latitude were computed using the values obtained from this simulation study, assuming that a reasonable estimate of uncertainty of measurements on-board the spacecraft is $\Delta\psi = \Delta\lambda = \Delta E = 1$ mAs. The results of this computation were reported in the last columns of **Tables 1–12**.

Looking at the values $\Delta\theta''$ reported in these columns, it appears that the relative error of the aberrated apical latitude $\frac{\Delta\theta''}{\theta''}$ decreases with a decrease of the aberrated apical latitude, providing the lowest-order relative error values ranging from 10^{-7} to 10^{-9} using aberrated apical latitudes lesser than 45°. This result is in agreement with the previous result regarding the increase in accuracy of determining the spacecraft's aberrated velocity β'' which was obtained using quasars' aberrated apical latitude $\theta \leq 45°$.

6. Conclusions

In this chapter an inertial celestial reference frame represented by three quasars, at least, was described, which can be used for future interstellar space missions at relativistic velocities. The equations to determine the aberrated apical coordinates

of a spacecraft as a function of the astronomical coordinates of a set of quasars were derived from spherical astronomy.

In particular, a simulation to increase the accuracy in the determination of the aberrated coordinates of a relativistic spacecraft during an interstellar space mission was carried out. The uncertainty of measurements in navigation control can be minimized selecting the set of quasars. The accuracy of determining the aberrated velocity and the aberrated apical coordinates of a spacecraft increased significantly ($p < 0.01$) using an inertial reference frame formed by quasars with aberrated apical latitudes lower than 45°. This result suggests feasible design techniques for measurements of quasars' aberrated angular distances aboard the spaceship within a cone with the axis in the direction of motion of the spaceship and an angular aperture of 45°.

Further simulation was performed assuming that measurements of quasars' angular distances can be carried out on-board the spacecraft with accuracy within 1 mAs. The uncertainty of the aberrated apical latitudes of a spacecraft was obtained in this simulation providing small errors ranging from 10^{-7} to 10^{-9} using quasars' apical latitudes less than 45°.

Finally, further corrections can be carried out taking into account corrections to aberrated coordinates due to Doppler shift, secular aberration drift, and the expansion of the universe.

A. Appendix

Aberrated velocity and apical latitude of a spaceship as a function of quasars' aberrated apical latitude

Author details

Emanuele Calabrò
CISFA "Interuniversity Consortium of Applied Physical Sciences" (Consorzio Interuniversitario di Scienze Fisiche Applicate), Messina, Italy

*Address all correspondence to: e.calabro@yahoo.com

References

[1] N.A.S.A. A report by the solar system exploration division. T.O.P.S: Towards other planetary systems. 1993

[2] Dyson F. Project Orion the Atomic Spaceship 1957–1965. USA: Penguin Books; 2002

[3] Bond A et al. Project Daedalus—Report on the BIS starship study. Journal of the British Interplanetary Society. 1978;**31**:S1-S192

[4] Long KF, Obousy RK, Tziolas AC, Mann A, Osborne R, Presby A, et al. Project Icarus: Son of daedalus—Flying closer to another star. Journal of the British Interplanetary Society Daedalus. 2009;**62**(11-12):403-414. arXiv: 1005.3833v1

[5] Frisbee RH. Advanced space propulsion for the 21st century. Journal of Propulsion and Power. 2003;**19**(6): 1129-1154

[6] Piefer G. Advanced fusion for space application. Prepared for Neep 602. 2000

[7] Andrews DG. Interstellar transportation using today's physics. In: Joint Propulsion Conference & Exhibit; Huntsville, Alabama; 2003

[8] Calabrò E. Relativistic aberrational interstellar navigation. Acta Astronautica. 2011;**69**:360-364

[9] Ma C, Feissel M. Definition and realization of the international celestial reference system by VLBI astrometry of extragalactic objects. IERS Technical Note No. 23; International Earth Rotation and Reference System Service (Paris: Observatoire de Paris); 1997

[10] Thornton CL, Border JS. "Radiometric Tracking Techniques for Deep-Space Navigation", Deep-Space Communications and Navigation Series. USA: Jet Propulsion Laboratory, California Institute of Technology; 2000

[11] Downs DS. Interplanetary Navigation using Pulsating Radio Sources. In: NASA Technical Reports TR N74-34150; October 1974. pp. 1-12

[12] Sheikh SI, Pines DJ, Ray PS, Wood KS, Lovellette MN, Wolff MT. Spacecraft navigation using X-ray pulsars. Journal of Guidance, Control, and Dynamics. 2006;**29**(1):49-63

[13] Sheikh SI, Golshan AR, PinesDJ. Absolute and relative position determination using variable celestial X-ray sources. In: 30th Annual AAS Guidance and Control Conference; 2007. pp. 855-874

[14] Ashby N, Howe DA. Relativity and Timing in X-ray Pulsar Navigation. IEEE; Contribution of the U.S. Government; 1-4244-0074-0/06; 2006

[15] Ma C et al. The international celestial reference frame as realized by very long baseline interferometry. The Astronomical Journal. 1998;**116**(1): 516-546

[16] Fey AL, Ma C, Arias EF, Charlot P, Feissel-Vernier M, Gontier AM, et al. The second extension of the international celestial reference frame: ICRF-EXT.1. Astronomical Journal. 2004;**127**:3587-3608

[17] Ma C, Arias EF, Bianco G, Boboltz DA, Bolotin SL, Charlot P et al. The second realization of the international celestial reference frame by very long baseline interferometry. IERS Technical Note No. 35; International Earth Rotation and Reference System Service (Frankfurt am Main: Verlag des Bundsesamts fur Kartographie und Geodasie) 2009

[18] Semyonov OG. Radiation hazard of relativistic interstellar flight. Acta Astronautica. 2009;**64**:644-653

[19] Hewitt A, Burbidge G. A revised and updated catalogue of quasi stellar objects. The Astrophysical Journal Supplement Series. 1993;**87**:451-947

[20] Green RM. Spherical Astronomy. New York, USA: Cambridge University Press; 1985

[21] Calabrò E. Interacting winds in eclipsing symbiotic systems. The case study of EG Andromedae. Journal of Astrophysics and Astronomy (JOAA). 2014;**35**(1):69-85

[22] Harwit M. Astrophysical Concepts. New York, USA: Springer-Verlag; 1988